UNIVERSITY OF CALIFORNIA

Santa Barbara

Application of micro-CT and Elliptic Fourier Analysis on Molar Outline Shape for Group Discrimination of Notoungulates

A thesis submitted in partial satisfaction of the

requirements for the degree Master of Science in Earth Science

by

Jackson Mitchell

Committee in charge:

Professor Andy Wyss, Chair

Professor Susannah Porter

Professor Sam Sweet

June 2016

The thesis of Jackson Mitchell is approved.

_____

Susannah Porter

_____

Sam Sweet

_____

Andy Wyss

June 2016

ACKNOWLEDGEMENTS

Foremost, I would like to express my profound gratitude to my advisor, Professor Andy Wyss, for his omnipresent support and advice (academic and other).

I would like to thank Ana Balcarcel from the American Museum of Natural History for kindly providing me with many of the samples used in the current work.

My final thanks go to the friends who motivated me throughout my time at UCSB: Elisabeth Norris, Jared Tuttle, and Noah Kimmes.

ABSTRACT

Application of micro-CT and Elliptic Fourier Analysis on Molar Outline Shape for Group Discrimination of Notoungulates

By

Jackson Mitchell

Mammal teeth commonly possess a crown shape that is unique to each species, and, as a result, taxonomic identification of mammals relies heavily upon dental analysis. Ever-growing (hypselodont) cheek teeth, acquired convergently within numerous lineages of Cenozoic (66 Ma – present) mammals, retard wear associated with abrasive diets. Four major groups of notoungulates, a diverse group of extinct South American herbivorous mammals that flourished during the Cenozoic, acquired hypselodont cheek teeth. Simplification of crown morphology is a developmental consequence of hypselodonty, leaving tooth crown outline as a potential metric for taxonomic identification. Although crown outline is prone to change during ontogeny, the inclusion of all possible crown outlines along the height of the tooth may effectively capture intraspecific variability. This study tests the power of crown outline shape analysis to discriminate among notoungulate genera/species. Micro-computed tomography, a non-destructive technique to visualize the internal structure of materials, was used to scan eight notoungulate specimens from five genera. From those eight specimens, 18 molars were reconstructed and analyzed. Teeth were sectioned digitally to ascertain how tooth outline would have changed during wear. Sections parallel to the occlusal surface for each tooth were subjected to elliptic

Fourier analysis (EFA) to compare outline shape. Results indicate that tooth crown outline can reliably discriminate among notoungulate groups.

TABLE OF CONTENTS

LIST OF FIGURES

INTRODUCTION

Traditional phylogenetic and taxonomic studies of mammalian fossils rely heavily on teeth for two reasons. First, due to their hardness, teeth are the most commonly preserved mammalian tissue. In fact, many extinct mammals are known only from isolated teeth (Kaiser et al., 2013). Second, the occlusal morphology of mammalian cheek teeth is generally complex and highly diverse, allowing taxonomic identification (Ungar, 2010). Despite the potential utility of mammal teeth, they are not without caveats. Teeth begin to wear soon after erupting into the oral cavity. Because of the heterogeneous composition of teeth, wear often results in a change of shape. In many groups this shape change is subtle, and for taxa that possess a robust fossil record, the shape variability is well documented (Rensenberger, 1973). Taxa with simplified occlusal morphologies and limited fossil records (e.g., some notoungulates) pose particular challenges because the intraspecific variability in tooth shape is not well known. Two notoungulate individuals of the same species may have dissimilar tooth crown morphologies, due to variability in tooth wear from either behavioral or age differences. Thus, in some mammalian groups, crown morphology may not be suitable for taxonomy.

Notoungulates, a group of extinct herbivorous mammals endemic to South America, were one of the first groups of mammals to acquire high-crowned (hypsodont) teeth (defined as the crown height to width ratio exceeding one). Hypsodonty is a recurring trend among Cenozoic mammals, presumably an adaptation to extend the functional longevity of teeth in response to high rates of

tooth wear (Koenigswald, 2011). High-crowned cheek teeth developed evolutionarily through the ontogenetic delay in the formation of roots, the point at which tooth height becomes fixed (Fortelius, 1985). By delaying root formation, the enamel- and dentin-forming organs at the base of the tooth deposit crown material over an extended period. If the root formation is delayed to the point of never occurring, that tooth effectively becomes rootless or open-rooted (hypselodont).

Hypselodonty has evolved many times in mammals, an outstanding example being the enlarged anterior teeth of modern rodents and lagomorphs (Ungar, 2010). Although the cheek teeth of most extant ungulate groups are hypsodont, hypselodonty is limited to the notoungulates and an extinct rhinocerid, *Elasmotherium,* among ungulates (Madden, 2014). During the developmental transition from hypsodonty to hypselodonty, the enamel-forming organs at the base of the teeth retreat to the perimeter of the tooth. The lack of enamel formation in the tooth interior early in development results in a highly simplified occlusal morphology once the tooth begins to wear.

Tooth wear occurs on the occlusal surface, the plane which faces the opposing tooth row. As the occlusal surface wears, the sides of the teeth are unchanged (Skogland, 1988). Particularly for hypsodont/hypselodont taxa, a large portion of the cheek teeth beyond the crown is unaffected by tooth wear (until it is erupted and eroded at the occlusal surface); hence, the outline may be the only stable metric of tooth shape that remains. Many paleontological studies depend on the accurate

assessment of dental morphology, thus, the ability to make predictions about the effects of tooth wear is of paramount importance.

This study aims to answer two questions. First, can tooth crown outline be used for taxonomic identification of notoungulate molars? Second, is there a perceptible change in outline shape along the height of notoungulate molars? Micro-computed tomography (micro-CT) is employed to view tooth outline at multiple levels along crown height in a non-destructive manner. A series of crown outlines, representing the occlusal outline at successive wear stages, were extracted from each notoungulate molar and analyzed using elliptic Fourier analysis (EFA). EFA has an advantage over other outline analysis methods in that it normalizes each outline for variability in size, rotation, and location. The matrices of elliptic coefficients were submitted to a principal components analysis to reduce the dimensions of multivariate analysis. Further analyses, canonical variates analysis (CVA) and a multivariate analysis of variance (MANOVA), were employed to discriminate between notoungulate genera based on molar outline shape.

If successful, this study will enable a much greater sample size to be used in many paleontological studies. Often, teeth exhibiting even moderate wear are discarded for taxonomic analysis, limiting the sample size for potential studies (Hopson, 1980; Gallina & Aspesteguia, 2011). Past studies have completed basic taxonomic identification of mammal molars using crown outline analysis; however, none have taken into account the susceptibility of crown outline to change with wear.

The inclusion of the entire range of crown outlines possible for each tooth may provide a means to supplement studies in which sample size/quality is limited.

BACKGROUND

Interpreting the Mammalian Fossil Record Through Teeth

With a few notable exceptions, most fossil vertebrate taxa are known from little more than a handful of skeletal fragments, often teeth. The external surfaces (and, sometimes, internal surfaces) of mammalian teeth are composed of enamel (97% hydroxyapatite), the hardest and most mineralized tissue in the body (Ungar, 2010). Because of their durability, teeth are one of the most commonly preserved body parts in the mammalian fossil record—a fortunate circumstance given that teeth yield considerable information about the organism that bore them (Jernvall, 2002).

Dental anatomy provides insights into an organism's diet, behavior, and phylogenetic placement (Billet, 2011; Nievelt & Smith, 2005; Ungar & Sponheimer, 2011). The unworn surface of teeth is the most phylogenetically informative (M'kikera & Ungar, 2003). An unworn tooth condition, however, is preserved infrequently because it is a momentary stage in a lifetime full of wear, degradation, and, ultimately, shape change. Shortly after erupting from the gingiva, teeth are abraded by food particles and the opposing tooth (Kullmer et al., 2009). When abundant specimens are available (as with modern and some fossil taxa), it is straightforward to track the change in crown morphology through wear (Dennis et al., 2004; Ungar & Williamson, 2000). For fossil taxa known from few and/or highly fragmentary specimens, the reliance on unworn teeth is problematic. Unfortunately, many notoungulate species are not known from unworn teeth (Strömberg et al., 2013).

Tooth wear occurs on the occlusal surface, paradoxically, the location that is most used for taxonomic identification. While the occlusal shape is altered during wear, the shape of the remainder of the tooth remains stable. During mastication, wear does not occur on the lingual and labial edges of teeth, preserving their unworn, genetically predetermined shape. Accordingly, the present study focuses on the shape analysis of tooth outline, rather than the occlusal surface.

Notoungulates

Notoungulates are a taxonomically and morphologically diverse group of herbivorous mammals endemic to South America. During most of the group's existence (57 Ma – 11 ka), South America was an island continent, until the formation of the Isthmus of Panama (3 Ma) allowed terrestrial biotic interchange between North America and South America (Woodburne et al., 2014). From the rhino-sized Toxodontia to the rabbit-sized Typotheria, notoungulates occupied a broad range of ecological niches. The first notoungulates appear in the fossil record early in the Cenozoic (57 Ma) and experienced a radiation at the Eocene-Oligocene boundary (33 Ma) (Paula Couto, 1952). This transition is marked by numerous changes in dental morphology that persisted for the remainder of the group's history (Reguero et al., 2010). While the monophyly of notoungulates is well-supported, relationships among many subgroups are less clear (Billet, 2011). Past studies of notoungulate phylogeny relied on occlusal dental morphology and, less frequently, the postcranial skeleton (Billet, 2011; Cifelli, 1993; Croft et al., 2004). Because of

their diversity, abundance, and long stratigraphic range, notoungulates are a key group for the study of mammalian evolution on the continent.

Hypsodonty

One of the most conspicuous features of South American mammals is the repeated acquisition of hypsodonty (high-crowned teeth); as many 26 clades independently evolved hypsodonty (Madden, 2014). Hypsodonty is thought to be a response to environmental conditions of high tooth wear, increasing dental durability (Williams & Kay, 2001). Curiously, the appearance of hypsodonty in in South American mammals (38 Ma) antedates that in mammals from other continents by roughly 10 myr (Madden, 2014). The exact evolutionary pressures favoring hypsodonty, especially its early acquisition among notoungulates, are still debated.

High-crowned teeth are most common among herbivorous mammals, particularly grazers. Grasses require a large amount of chewing to break their cell walls and acquire nutrients; they also have a low caloric density, increasing the volume of food consumed by grazers, relative to non-grazing herbivores (Williams & Kay, 2001). An early hypothesis linked the origin of hypsodonty with the spread of grasslands, and the associated ingestion of phytoliths (McNaughton & Tarrants, 1983; MacFadden, 1997). Recent studies reveal that phytoliths lack the hardness necessary to erode teeth (Sanson et al., 2007; Lucas et al., 2014). Another hypothesis proposed that the formation of the Andes mountain range played a role in the evolution of hypsodonty (Pascual & Jaureguizar, 1990). During the formation of the Andes, the increased elevation of the range would have raised regional erosion rates (Madden,

2014). A portion of the eroded sediment would have ended up covering plant surfaces, eventually being ingested by grazing herbivores and contributing to tooth wear. Also, the volcanism accompanying Andean mountain building produced ash, further covering plants with erosive material (Stirton, 1947).

The most widely accepted view is that the exogenous grit and dirt that attaches to plants in open-habitats, often, but not necessarily, in grasslands, is the likeliest driving force behind the attainment of hypsodonty in mammals (Mendoza and Palmqvist, 2008; Jardine et al., 2012; Strömberg, 2011; Strömberg et al., 2013). Regardless of the precise causes, South American mammals show a substantial increase in tooth crown height throughout the mid-late Cenozoic (30 Ma – present). Few groups exemplify this trend better than notoungulates, 75% of which acquired hypsodonty by 30 Ma (Madden, 2014).

Hypselodonty

The progression from low-crowned (brachydont) to high-crowned (hypsodont) teeth is thought to be related to heterochrony, the change in developmental rates. A delay in the onset of root formation, the point at which tooth height is set, prolongs the production of dentin and enamel, increasing the height of the crown (Renvoisé & Michon, 2014). Thus, the stepwise increase in tooth crown height in herbivorous mammals during the Cenozoic may stem from the progressive delay of root formation. At some point, root formation is delayed to the point that they fail to form altogether, resulting in ever-growing teeth (hypselodonty). In short, hyselodonty is merely an extreme case of hypsodonty. Hypsodonty evolved in six

clades of notoungulates, four of which proceeded to attain hypselodonty (Toxodontidae, Interatheriidae, Mesotheriidae, Hegetotheriidae). Three of these four groups are represented in the current study (Toxodontidae, Interatheriidae, and Hegetotheriidae).

The acquisition of hypselodonty is accompanied by a simplification of occlusal morphology. By reducing the extent of the enamel-forming organ, isolated enamel fossettes within the perimeter of the tooth, typically responsible for occlusal complexity, are lost (Madden, 2014). The reduction of the enamel-forming organ occurs early in development; thus, moderately worn hypselodont teeth invariably have a featureless occlusal surface.

Computed Tomography

Classically, it has been difficult to assess the changes in cheek tooth outline in hypsodont taxa, because a large portion of the crown is embedded within the upper and lower jaws. Past methods relied on destructive techniques to create physical cross-sections of each tooth to view the hidden structure, heavily limiting the use of samples for future studies (Bourque et al., 1978; Luckett, 1993; Kaiser & Brinkmann, 2006). X-ray micro-computed tomography (CT) provides a means of studying the morphology of concealed portions of the dentition non-destructively. Digital reconstructions of scanned fossils can be easily shared, promoting collaboration with multiple colleagues simultaneously.

Micro-CT scanning is increasingly being used to study fossil vertebrates (Kono, 2004; Suwa & Kono, 2005; Olejniczak et al., 2008; Ni et al., 2010; van Dam

et al., 2011). A key advantage of computed tomography over traditional sectioning is the ease with which internal and external anatomy of fossil organisms can be viewed, obviating the need for extensive fossil preparation/destruction. In micro-CT analysis x-ray attenuation is measured through a solid object, reflecting spatial changes in density and mean atomic number of the specimen (Abel et al., 2012). The differential attenuation of x-rays allows the complex internal (and concealed external) structure of hypsodont teeth to be documented in detail (Fig. 1).

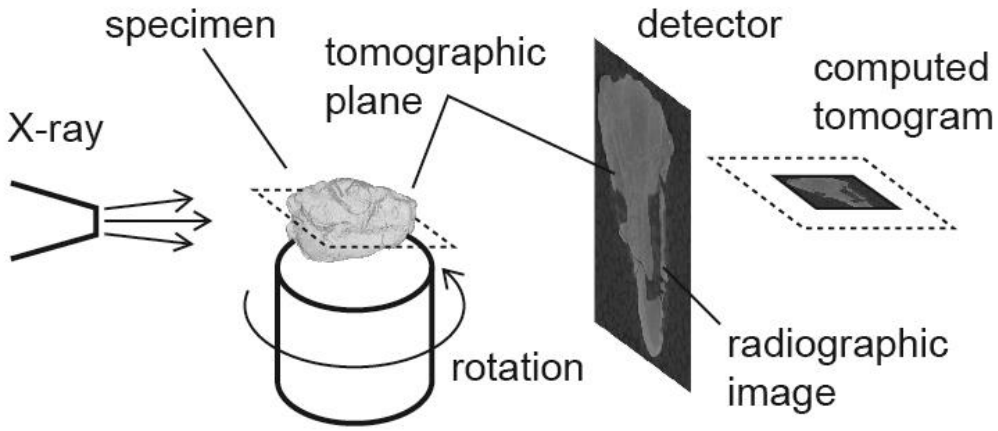

Figure 1. The basics of computed tomography

Shape Analysis

Biological shape analysis examines anatomical differences among taxa to describe their evolutionary history. From initially qualitative descriptions, shape analysis slowly became a rigorous quantitative matter over the past century (Thompson, 1942; Young et al., 1974). Traditional morphometrics use basic measurements of length, depth, and width, limiting analysis to size metrics (Strauss & Bookstein, 1982). The modern definition of shape within morphometrics is "the

geometric information that remains when location, scale, and rotational effects are removed" (Kendall, 1977). An important advance in shape analysis was the advent of geometric morphometrics, a shape analysis technique that quantifies shape variance independent of size (Zelditch, 1998).

The most commonly employed form of geometric morphometrics places anatomical landmarks onto specimens within a Cartesian coordinate system. The location of landmarks are then compared, providing a measure of variation in form among and within groups (Zelditch et al., 2012). The landmark system relies on discrete, homologous points. The prerequisite of homology limits shape analysis to structures that can be consistently located, precluding shape analysis of many biologically interesting structures in which homology is uncertain. Curves and outlines, in particular, are impossible to compare using traditional landmark geometric morphometrics.

Among the various methods used to analyze outlines, elliptic Fourier analysis (EFA) has been particularly successful. EFA, first proposed by Kuhl and Giardina (1982), decomposes two-dimensional, closed outlines (delineated by x,y coordinates) into a set of harmonic ellipses, each of which is defined by four coefficients (elliptic Fourier descriptors; EFDs). EFA of each outline in the sample produces a matrix of EFDs which describe the shape. The matrix of EFDs is then used in subsequent multivariate analyses, most commonly a principal components analysis (PCA). A combined EFA and PCA approach has been applied in many zoological and botanical studies of outline shape including: tree crowns (Hâruta, 2011), primate mandibles

(Daegling and Jungers, 2000), cereal grains (Mebatsion et al., 2011), leaves (Adebowale et al., 2012), cucumbers (Shimomura et al., 2016), and fish otoliths (Tracey et al., 2006; Lord et al., 2012).

EFA has had only limited application in analyses of mammal teeth, generally in relation to the occlusal shape. Renaud et al. (1996) used Fourier analysis to examine the shape change in murid molars, discovering a discontinuous pattern of change through time. Bailey and Lynch (2005) used shape differences to distinguish the cheek teeth of Neanderthals and anatomically modern humans, with successful classification rates (86.4%). Kaifu et al. (2015) used EFA to compare molars of *Homo florensis* to related hominin lineages. Renaud and Michaux (2004) successfully discriminated *Malpaisomys insularis* from contemporaneous fossil rodents using an EFA of molar outline.

While there have been a number of studies that utilize EFA to analyze tooth outline, the current study is the first to apply this method to examine outline shape change throughout the wear history of each tooth. As the occlusal surface wears, a new section of the tooth is erupted, exposed, and subsequently eroded. Assuming that eruption rates for notoungulates are similar to related ungulate groups (0.1-1.0 mm/day) (Madden, 2014), it is unlikely that the occlusal outline for an individual will exactly match that of another individual of the same species. Analyzing the full range of potential occlusal outlines within a single tooth, which reflect different wear stages, accounts for the variety in outline shapes possible for a group.

MATERIALS AND METHODS

Study Taxa

Fossil specimens were collected in mid-late Cenozoic (30 Ma – present) rocks of South America. The sample consists of eight notoungulate skulls representing five genera (Table 1). Specimens were selected due the hypselodonty of their cheek teeth. Of the four groups of notoungulates that acquired hypselodonty, three are represented in the present study (Hegetotheriidae, Toxodontidae, and Interatheriidae). From the eight individuals in the sample, 18 molars were selected for detailed analysis. When possible, molars from the upper right dentition were chosen. In AMNH 9260, which lacked right-side dentition, left molars were used and mirrored to represent the right molars; a left and right molar of identical position (M3) from AMNH 9534 were used to test the assumption of left-right symmetry in outline shape.

Specimen	**Family**	**Accession Number**	**Teeth Used**
Adinotherium robustum	Toxodontidae	AMNH 9532	rM3
Adinotherium sp.	Toxodontidae	AMNH 9229	rM3
Hegetotherium mirabile	Hegetotheriidae	AMNH 9156	rM1 rM2 rM3
Paedotherium chapadmalensis	Hegetotheriidae	AMNH 45914	rM1 rM2 rM3
Protypotherium australe	Interatheriidae	AMNH 9534	lM3 rM1 rM2 rM3
Protypotherium australe	Interatheriidae	AMNH 9226	rM1 rM2 rM3
Protypotherium sp	Interatheriidae	AMNH 9260	lM2 lM3
Cochilius sp.	Interatheriidae	FMNH 3.22.99.974	rM2

Table 1. Specimens and teeth analyzed in this study. “r”=right tooth, “l”=left tooth, “M”=upper molar.

Computed Tomography

X-ray micro-computed tomography was carried out at two facilities. The American Museum of Natural History used a GE phoenix v|tome|x s240 system to scan the following specimens: AMNH 9532, 9229, 9156, 45914, 9534, 9226, and

9260. The resulting raw data consist of 1024x1024 pixel arrays of 16-bit .tiff image stacks. The isometric voxel size (i.e., scan resolution) for each specimen is as follows (in millimeters): 0.14180311, 0.10693795, 0.08141302, 0.06360822, 0.06752787, 0.07980076, and 0.05666162, respectively.

The Penn State Center for Quantitative Imaging scanned FMNH 3.22.99.974 using an X-TEK x-ray system. The data consist of a 1024x1024 pixel, 16-bit .tiff image stack. The resulting voxel size for the scan is: x,y = 0.060 mm, z = 0.0690459.

Segmentation and Model Creation

The raw .tiff images, ranging from 1,373-2,042 images per scan, were stacked and scaled to make a volumetric reconstruction of each skull using Sed3D v. 2.3.1 (Scientific Computing and Imaging Institute, Salt Lake City, UT). A semi-automatic thresholding technique was applied to the volumetric data to separate the molars from the skull matrix. The segmented molars were saved as masks, highlighting the regions of interest present in the .tiff stacks. The masks were imported into 3D Slicer v. 4.5.0-1 (http://www.slicer.org/) and converted into stereolithographic models (.stl) for further analysis.

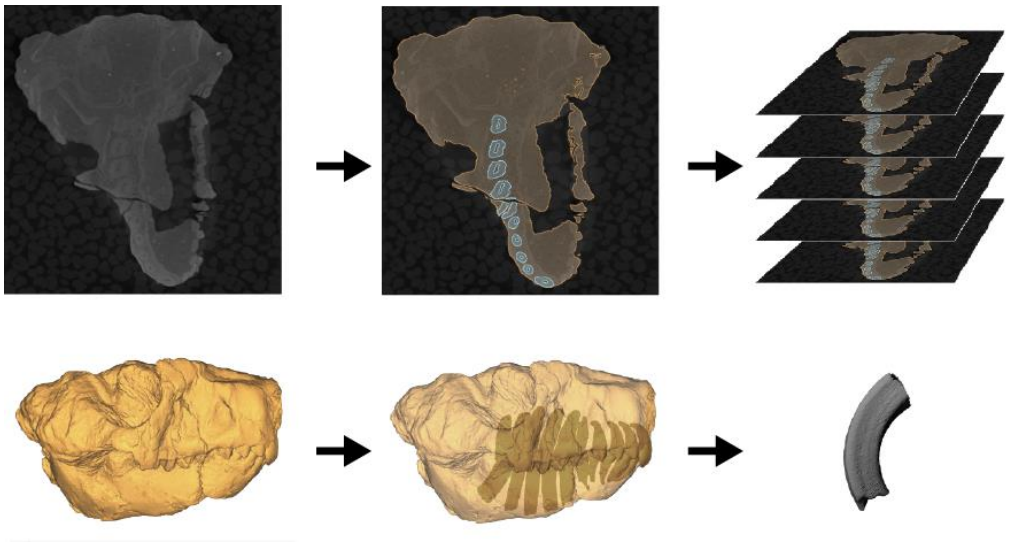

Figure 2. Molar segmentation and reconstruction process from raw CT data, using Seg3D.

Slice Acquisition

The modeled upper molars reveal a strong degree of (buccally-convex) curvature from the anterior perspective (Fig. 3). Assuming that the orientation of the present occlusal surface is constant, the curvature of the upper molars will be maintained throughout the lifetime of the teeth. To estimate the position of future occlusal planes, two lines were created to determine the intersection of the occlusal and apical planes (Fig. 3). From this intersection point, 10 equally-spaced planes were created and extended through the tooth. The occlusal and apical slices were determined visually, while the remaining slices were generated automatically. This method presumes that the position of the occlusal plane is fixed through wear. Ten, equally-spaced outlines were extracted as .jpg files from each of the 19 molars using Rhinocerous 3D v 5.0 (McNeel, 2010).

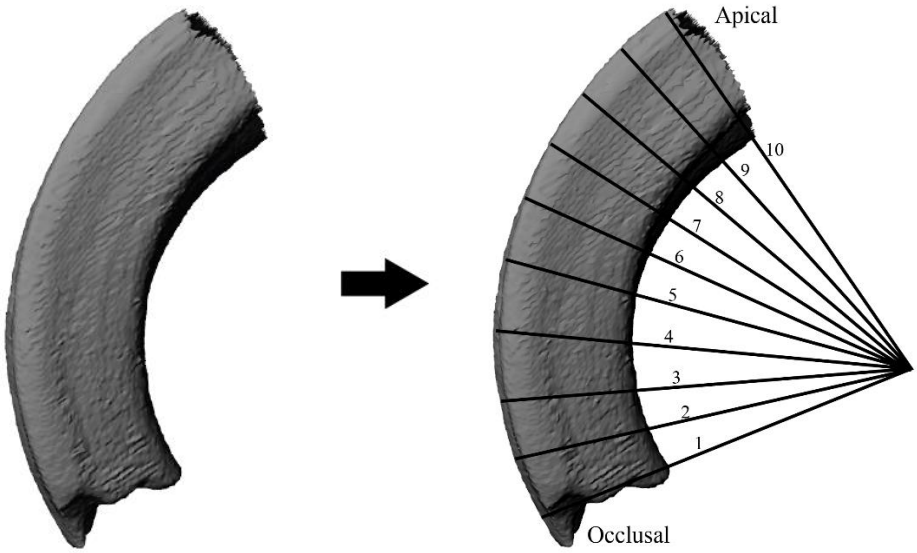

Figure 3. Outline orientation and numbering; anterior view of right M2 (AMNH 9534).

Shape Analysis

Tooth outlines were formatted to full color 24-bit bitmap (.bmp) images using ImageJ (Rasband, 1997). Images were binarized, converting the tooth contour into a black plane over a white background. These outline images were imported into SHAPE v 1.3 for elliptic Fourier analysis (EFA), the latter of which generated 40 harmonics for each tooth outline (Iwata & Ukai, 2002). SHAPE uses the Cartesian coordinates of the 2D outlines as inputs to create a chaincode, a quantitative representation of a line (Freeman, 1974). To determine the appropriate number of harmonics, the harmonic number was progressively increased until the tooth contour was adequately approximated (Fig. 4).

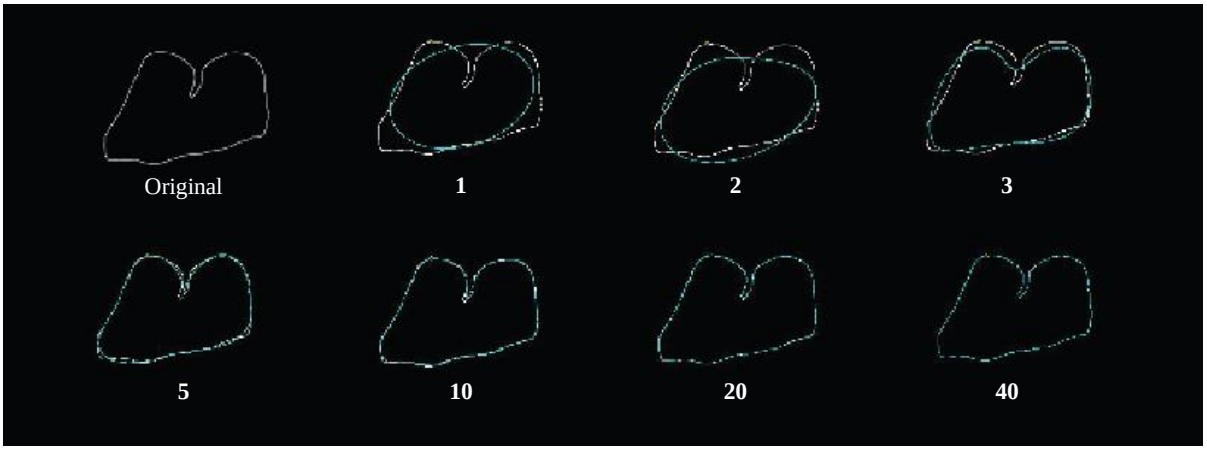

Figure 4. Tooth outline approximation with increasing number of harmonics.
Blue is the outline approximated by EFA, white is the true outline.

Each harmonic is composed of four coefficients, resulting in 160 coefficients per slice, the first three coefficients for the first harmonic being fixed. Fixing the first three coefficients as constants normalizes each tooth contour for changes in size, orientation, and location. The subsequent 157 coefficients describe the tooth outline for each of the 180 slices.

Statistical Analysis

Principal components analysis (PCA) was used to examine variance in the EF coefficient variance-covariance matrix. PCA reduced the 157 EF coefficients from each tooth slice into a smaller set of uncorrelated variables accounting for the dominant components of variation in the sample. The first three PCs were plotted against one another to view shape relationships among specimens. The effects of each PC on outline shape were visualized using an inverse Fourier transform.

A canonical variates analysis (CVA) was performed on the first seven principal components to examine group differences in outline shape. CVA is a

multivariate technique that uses linear combinations of variables to test whether two or more groups can be reliably discriminated (Fisher, 1936). Each tooth slice was assigned a number (1-5), specifying the genus involved. PC scores for each tooth slice were input into the CVA using PAST v 3.12 software (Hammer et al., 2001). The resulting eigenvectors were used to plot the PC scores onto canonical variate (CV) axes. The CV values are then used to test group discrimination. Within the CV analysis, a jackknife validation was performed on the same set of PC data. Jackknife validation excludes one slice at a time, discriminates the remaining data, and reclassifies the excluded data. A further CV assessment was conducted to test how reliably different molar positions could be distinguished within a genus.

A MANOVA (multivariate analysis of variance) was used to test the classification of each tooth outline into the correct genus. MANOVA uses dependent variables of two or more groups to assess whether the vectors of group means are sampled from the same population (Adebowale et al., 2012). The common metric of a MANOVA analysis, Wilk's λ, returns a value <0.0005 if the groups are well explained by the inputted variables (PC scores). The PC scores for each of the 180 slices, along with the group identifier, were analyzed via a MANOVA in PAST software.

RESULTS

Shape Analysis among Genera

Representative cross-sections of each of the 18 teeth examined reveal that each tooth outline is an oval variant, elongated in the anteroposterior plane (Fig. 5). The teeth are longest and straightest buccally. Despite similarities within specimens, no two slices are identical among the sample. The *Protypotherium* molars (9226, 9534, and 9260) all exhibit varying degrees of indentation lingually, while the *Paedotherium* teeth (45914) are well-rounded. The *Adinotherium* molars exhibit a pronounced posterior indentation and single, sharp lingual groove.

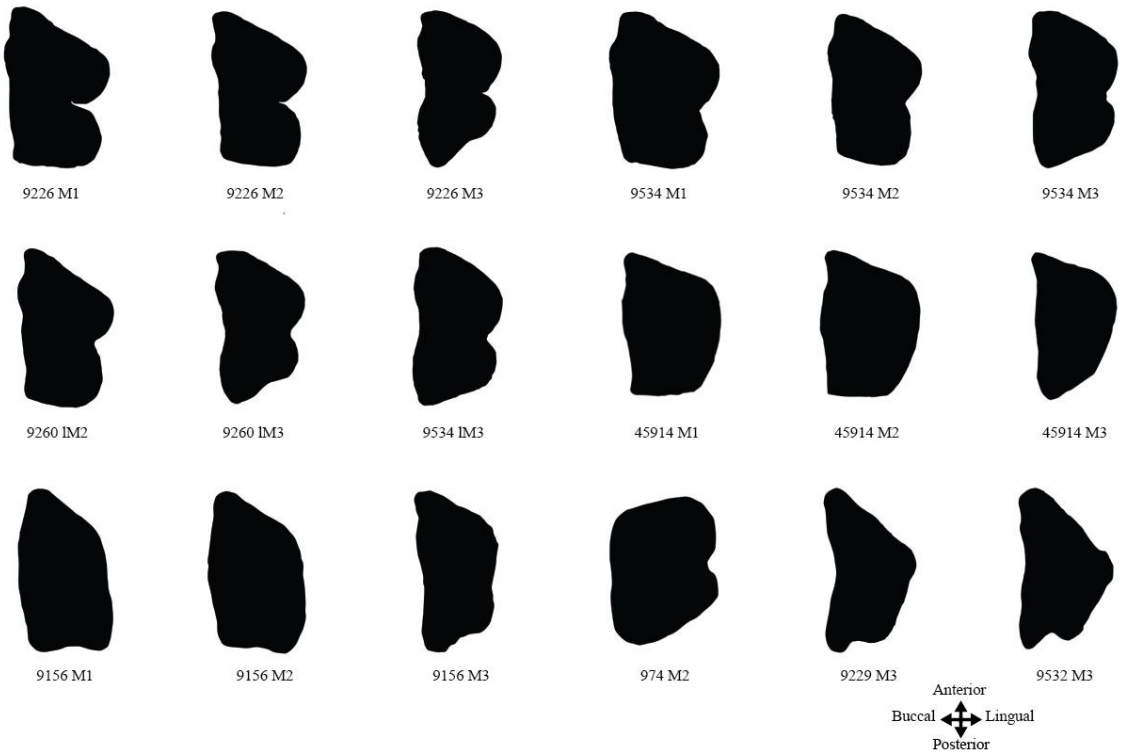

Figure 5. A single slice taken from each of the 18 teeth examined at approximately mid-height along the crown. Right teeth, unless otherwise noted.

Analysis of the EF coefficients from all 180 slices indicates that the first six PCs account for 94.4% of shape variance in the sample (Table 2).

Component	Eigenvalue	Proportion (%)	Cumulative Proportion (%)
1	8.07×10^{-3}	41.9	41.9
2	4.23×10^{-3}	21.9	63.9
3	2.57×10^{-3}	13.4	77.3
4	1.61×10^{-3}	8.42	85.7
5	1.08×10^{-3}	5.63	91.3
6	6.09×10^{-4}	3.17	94.4
7	4.00×10^{-4}	2.15	96.5
8	1.61×10^{-4}	0.846	97.4

Table 2. Eigenvalues and contribution of the first eight principal components

The effects of each PC on outline shape are shown in Fig. 5. The first PC describes the amount of lingual indentation; the second the amount of bucco-lingual compression (i.e., teeth with an increase in PC 2 have a more hourglass shape); and the third the orientation of occlusal symmetry (a high third PC value indicates a sharper anterior angle and an increase in the relative size of the antero-lingual protrusion, relative to the postero-lingual protrusion).

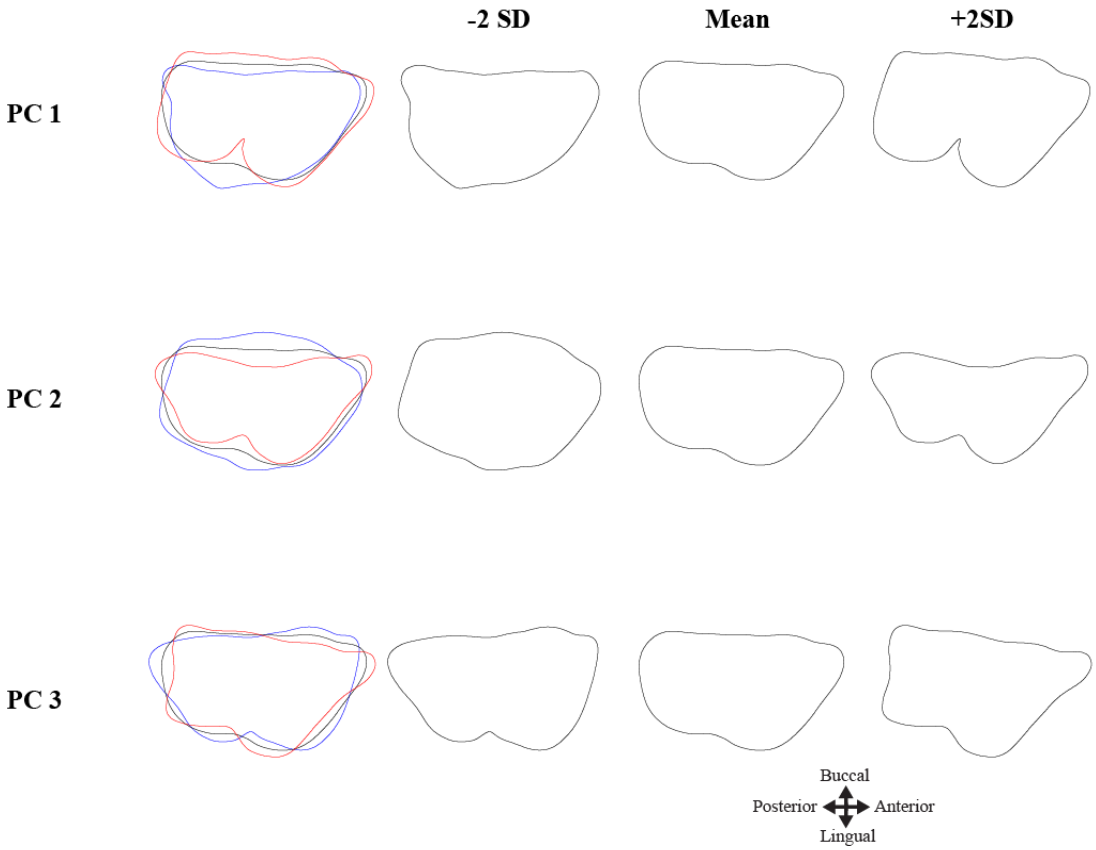

Figure 6. The shape variance explained by each PC. Blue is -2SD, red is +2SD.

The first three PCs were plotted against one another, grouped by genera (Fig. 7-9). Another set of PC plots separates specimens and tooth positions by color and symbol, respectively (Fig. 10-12).

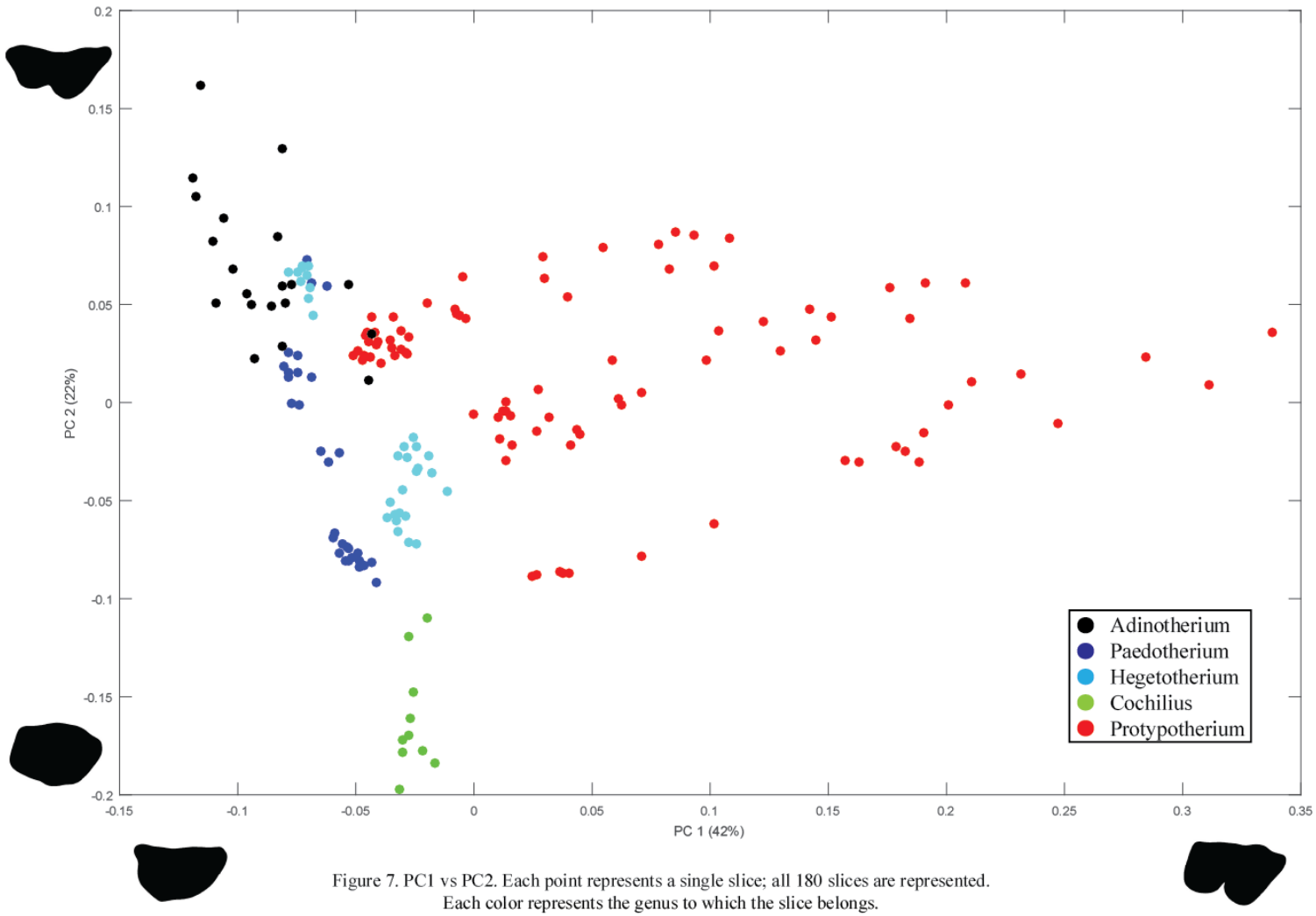

Figure 7. PC1 vs PC2. Each point represents a single slice; all 180 slices are represented.
Each color represents the genus to which the slice belongs.
Tooth contours indicate the shape of +-2SD for each PC.

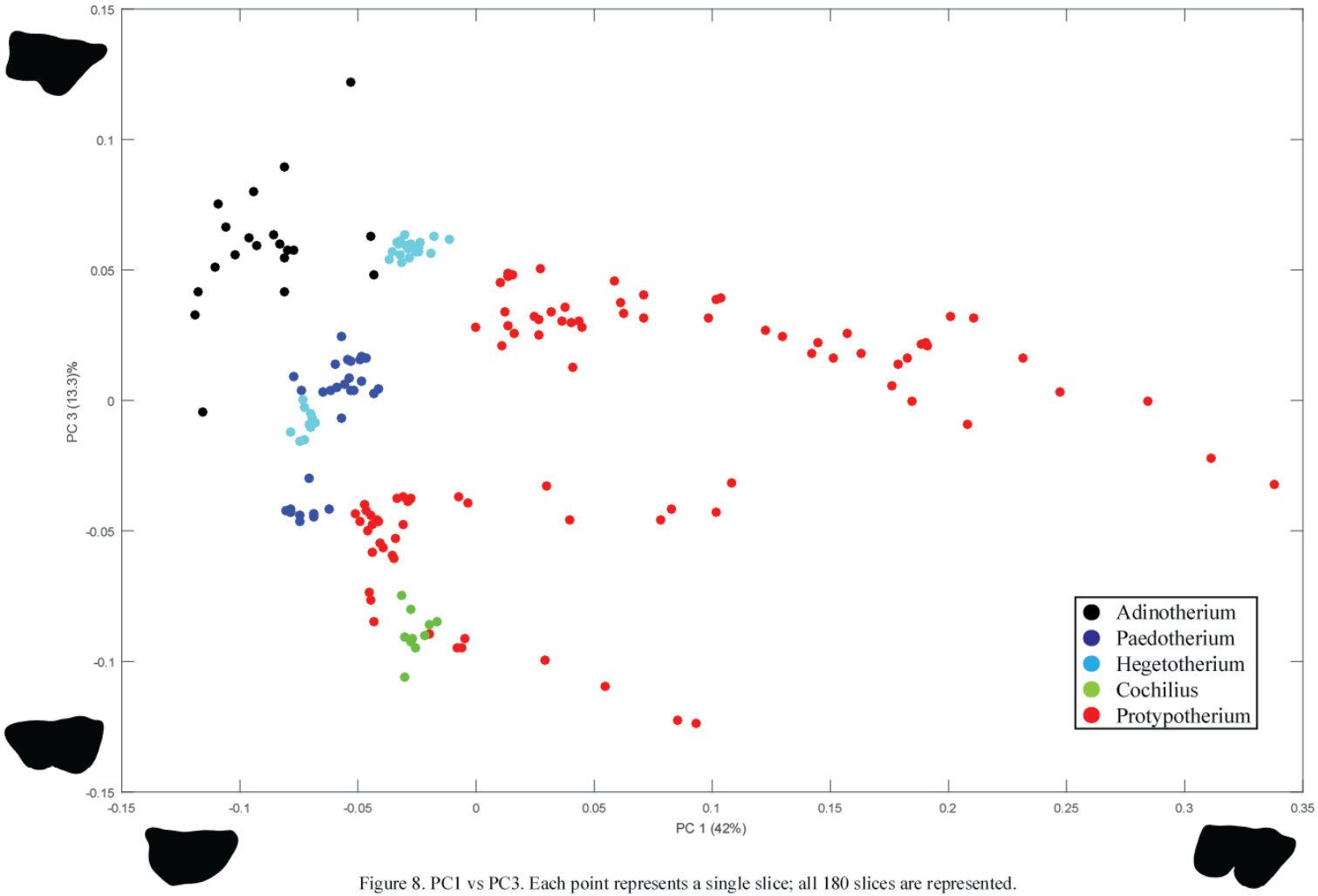

Figure 8. PC1 vs PC3. Each point represents a single slice; all 180 slices are represented.
Each color represents the genus to which the slice belongs.
Tooth contours indicate the shape of +-2SD for each PC.

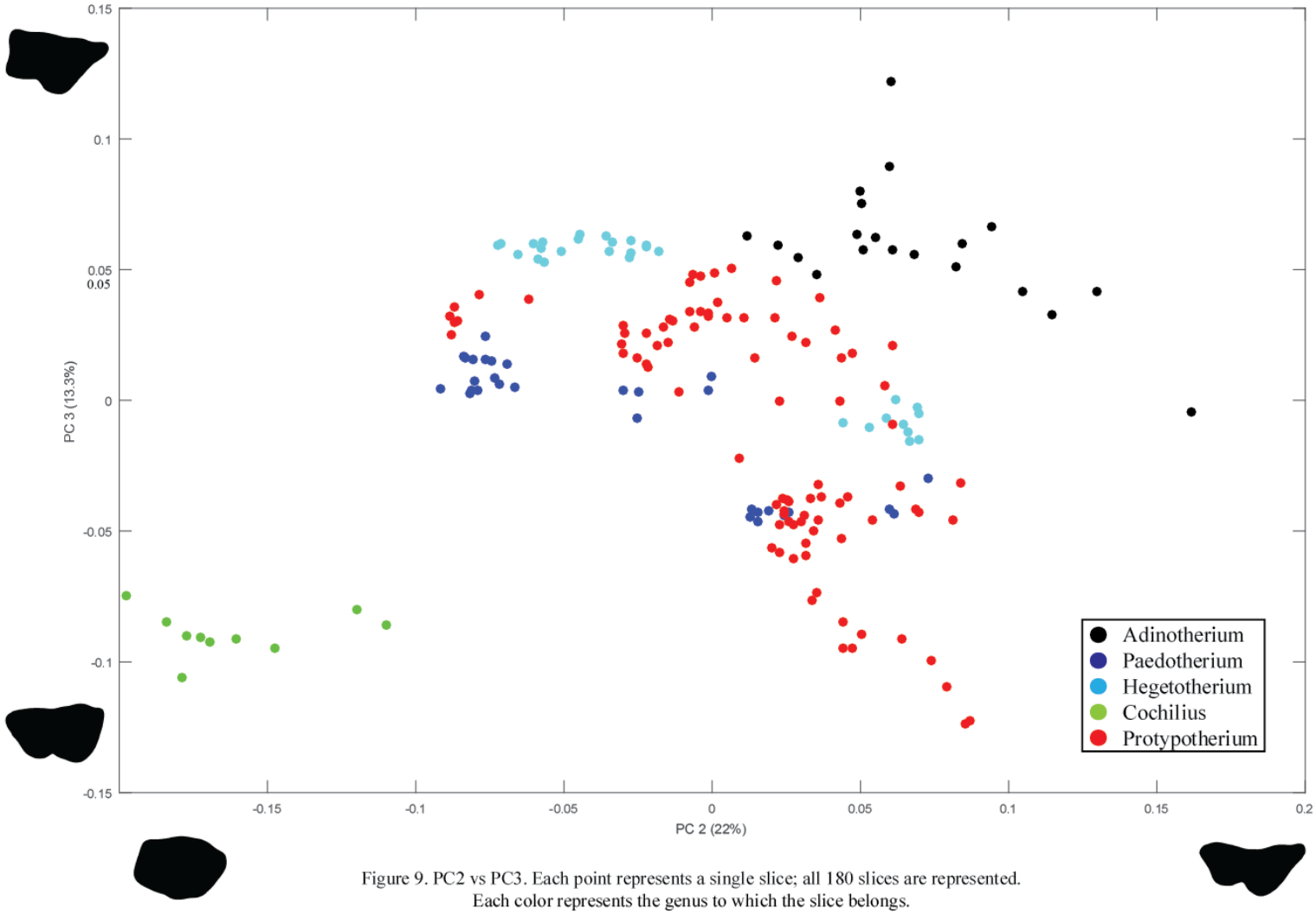

Figure 9. PC2 vs PC3. Each point represents a single slice; all 180 slices are represented.
Each color represents the genus to which the slice belongs.
Tooth contours indicate the shape of +-2SD for each PC.

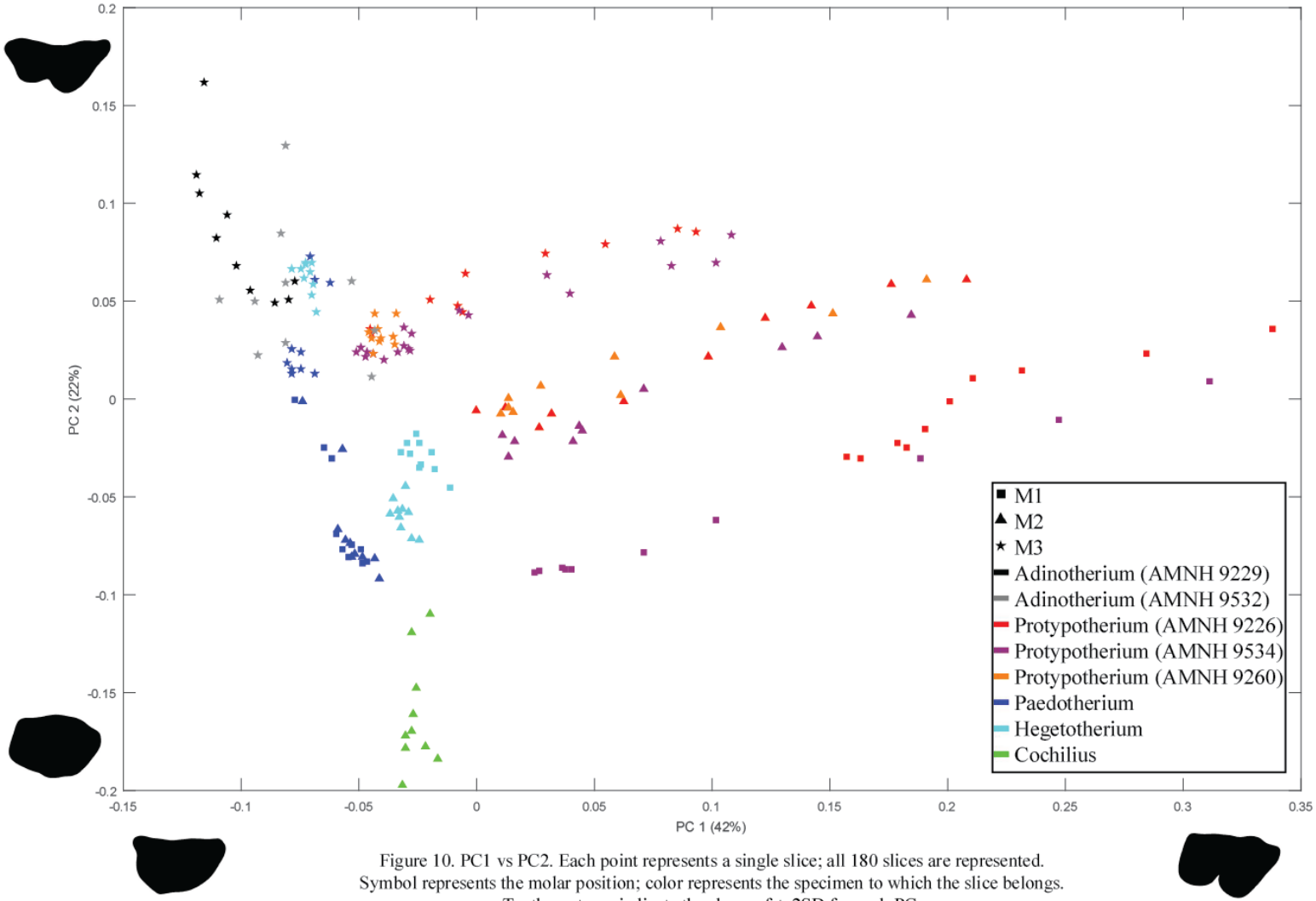

Figure 10. PC1 vs PC2. Each point represents a single slice; all 180 slices are represented. Symbol represents the molar position; color represents the specimen to which the slice belongs. Tooth contours indicate the shape of +-2SD for each PC.

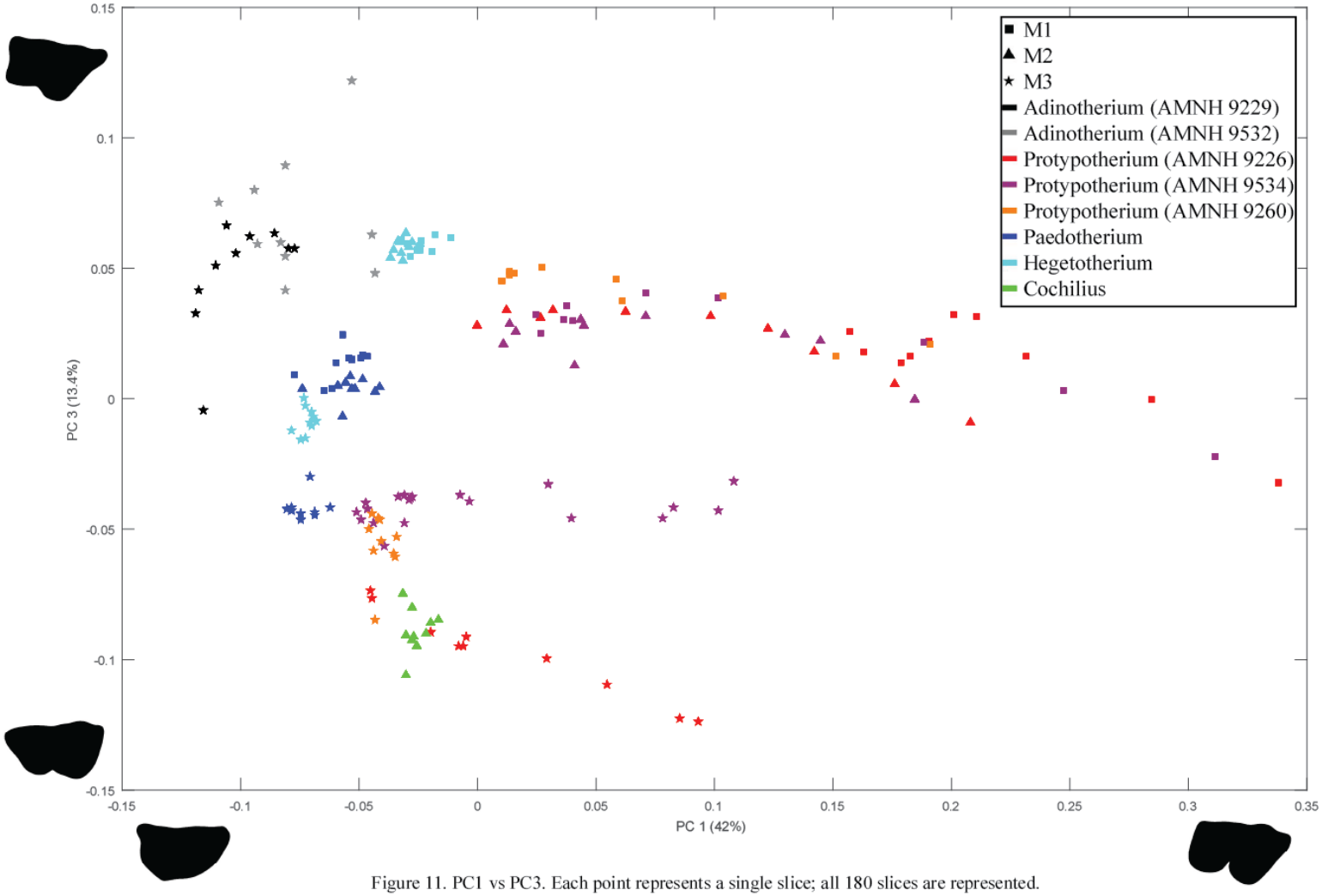

Figure 11. PC1 vs PC3. Each point represents a single slice; all 180 slices are represented. Symbol represents the molar position; color represents the specimen to which the slice belongs. Tooth contours indicate the shape of +-2SD for each PC.

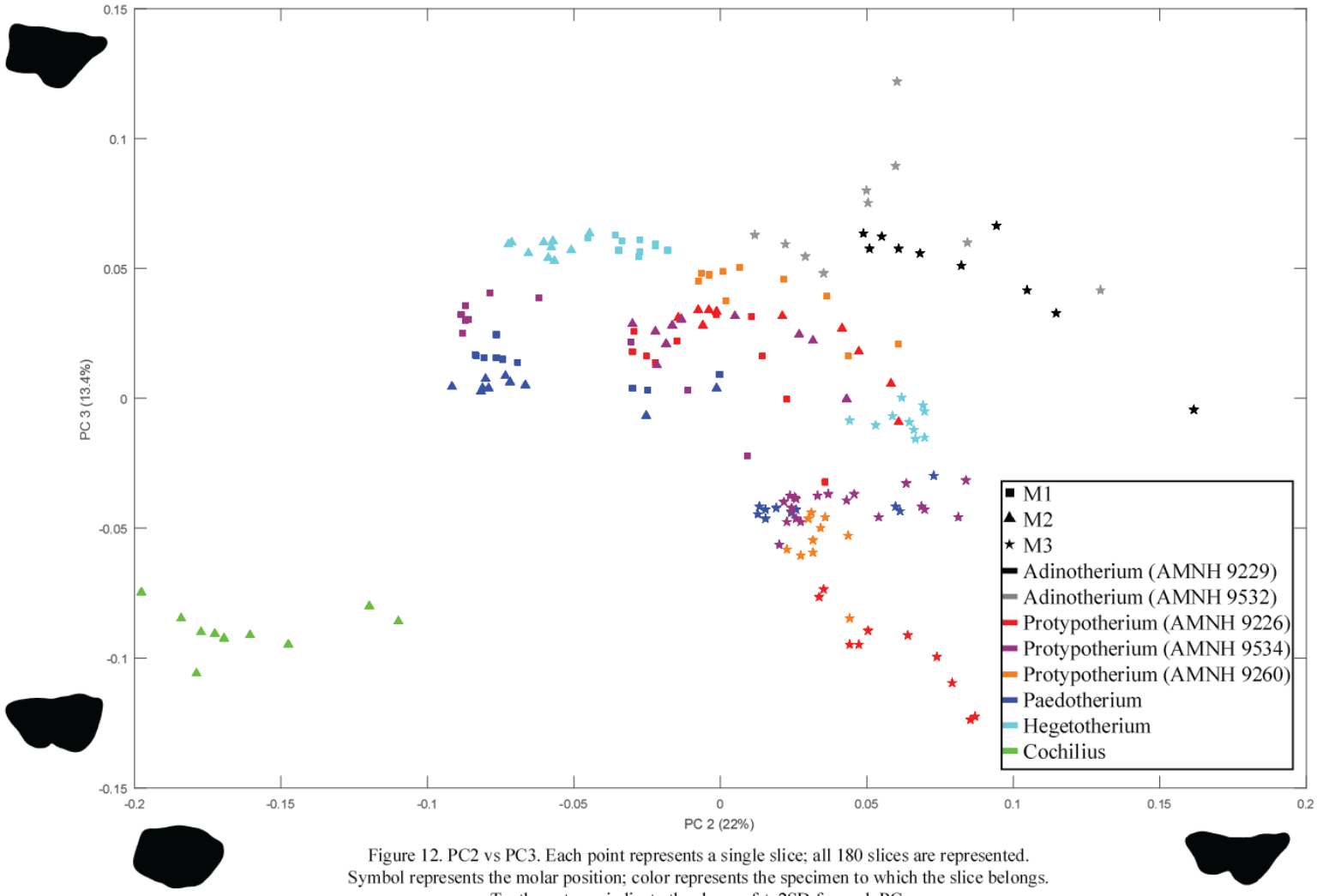

Figure 12. PC2 vs PC3. Each point represents a single slice; all 180 slices are represented. Symbol represents the molar position; color represents the specimen to which the slice belongs. Tooth contours indicate the shape of +-2SD for each PC.

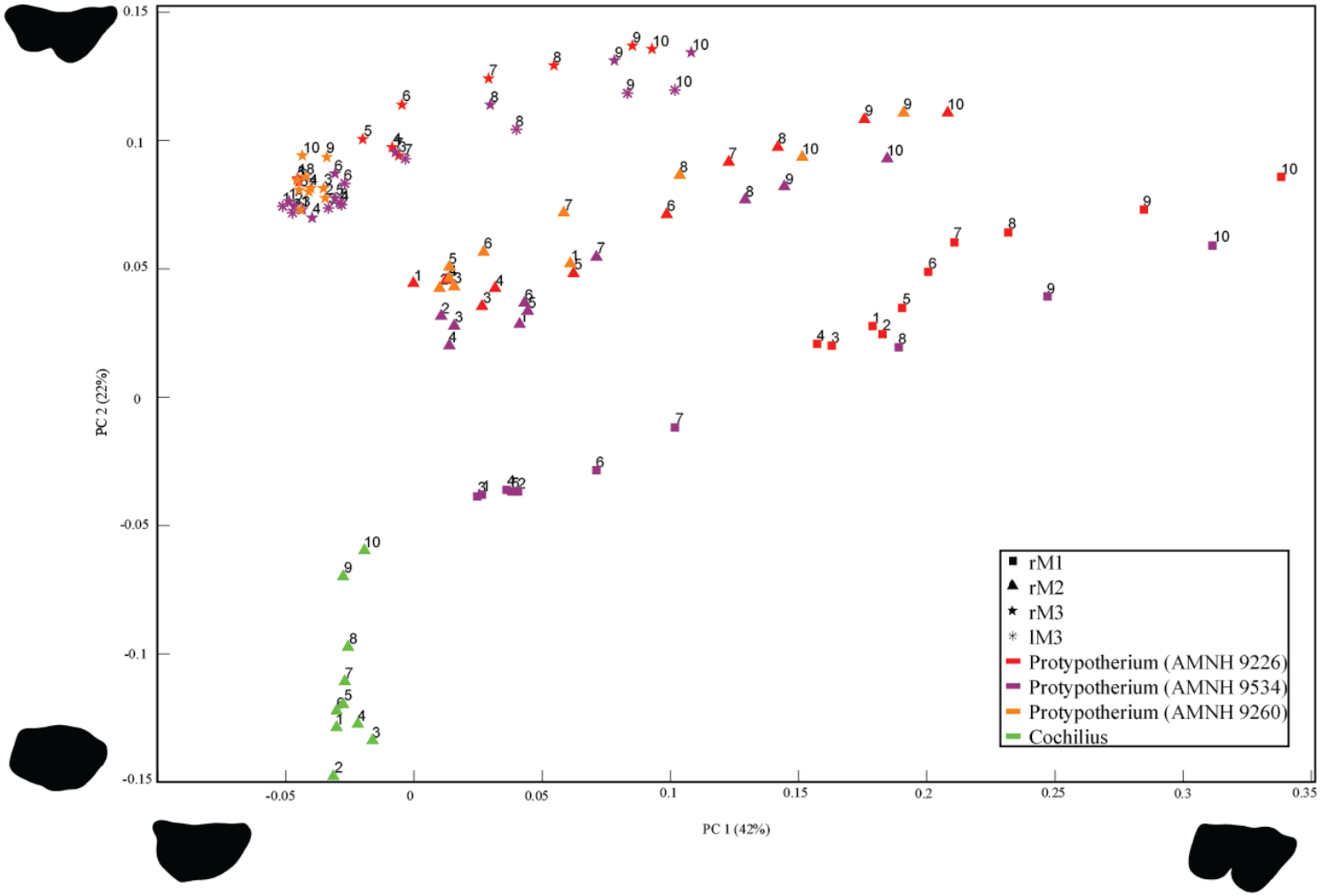

Figure 13. *Protypotherium* and *Cochilius* specimens isolated to show the change in outline along the height of each tooth. 10 slices per tooth. Symbol represents tooth position; color represents specimen; number represents slice position (1=occlusal, 10=apical; see Fig. 3).

The plots in Fig. 7-9 exhibit the shape variance among the outlines of different notoungulate genera. Although the *Protypotherium* molars span the greatest range of morphologic shape space, they nonetheless occupy a unique range within the sample. The ranges of *Hegetotherium*, *Paedotherium*, and *Cochilius* molars are more concentrated, while the *Adinotherium* molars have a moderate, yet distinctive, range of outline shapes.

The molars of *Protypotherium* (Fig. 10-12), red, orange, and violet points) occupy distinctly separate spaces. PC1 increases strongly and PC2 moderately toward the apical end (indicated by the slice number adjacent to each point in Fig. 13). This progression is consistent throughout the population of *Protypotherium* molars, with the exception in the mirrored left M3 of AMNH 9260. The M2 of *Cochilius* occupies a circumscribed area within each plot, with PC2 increasing apically (Fig. 13). The remaining teeth display no consistent trend from the occlusal plane to the apical plane.

Paedotherium and *Hegetotherium* molars appear as two separate populations within the shape space (Fig. 10-12; dark blue and cyan, respectively). In both genera, however, M3 is well-separated from the M1 and M2. M3 has a decreased score for PC1 and PC3, and an increased score for PC2, relative to the PCs of M1 and M2.

Statistical Results

Canonical variates analysis (CVA) clearly separates the genera along the canonical variates (CV) axes (Fig. 14).

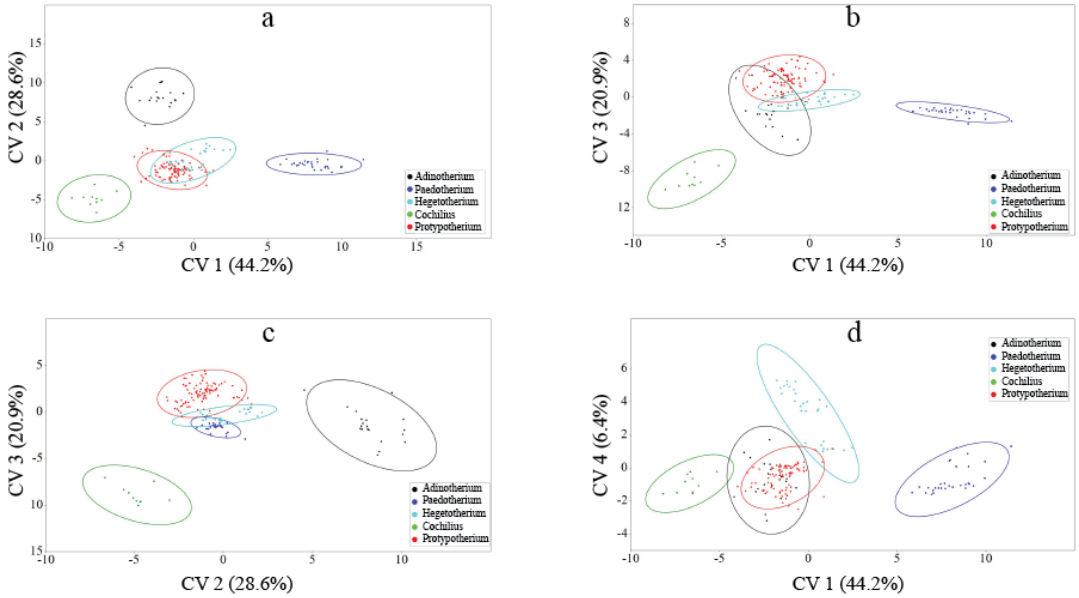

Fig. 14. CV axes with genus discrimination. a) CV1 vs CV2 b) CV1 vs CV3 c) CV2 vs CV d) CV1 vs CV4
Each dot represents a single slice. All 180 slices from 18 teeth are represented. Colors indicate the genus of each slice. Ellipses indicate the 95% confidence range for correct classification.

The CVA of the PC data correctly classified 100% of the slices into genera. The jackknifed cross-validation of the same data correctly classified 99.44% of the slices (a single *Protypotherium* molar outline was mistaken for a *Cochilius* molar).

MANOVA revealed significant differences in outline shape among the five genera (Wilk's λ=0.0002065, $p<0.0001$) from the first five PCs.

	Paedotherium	*Hegetotherium*	*Protypotherium*	*Cochilius*	*Adinotherium*
Paedotherium	-				
Hegetotherium	9.482E-24	-			
Protypotherium	8.136E-24	5.145E-31	-		
Cochilius	2.173E-19	3.532E-20	2.713E-39	-	
Adinotherium	1.641E-23	7.63E-23	3.275E-46	1.763E-	-

Table 3. Inter-genus molar outline shape differences from MANOVA of PC scores.

Molar Analysis within Genera

Among the specimens in which all three molars are represented (9226, 9534, 9156, & 45914), M3 is markedly different from M1 and M2. The posterior face of

M1 and M2 is oriented roughly bucco-lingually, while in M3 this surface is canted anteriorly. The success of the CV analysis for genus classification prompted a CV test to determine if tooth position was distinguishable within an already correctly-classified genus. The results of the CVA for tooth position discrimination can be seen in Fig. 15-16.

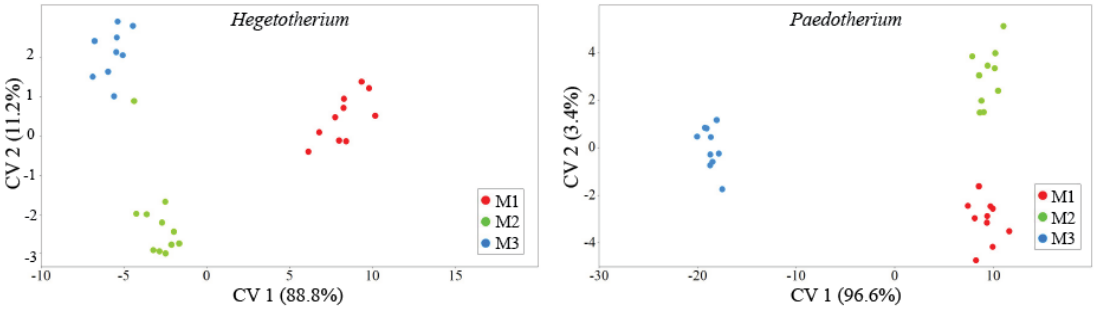

Figure. 15. CV axes of *Hegetotherium* and *Paedotherium* outline shape.

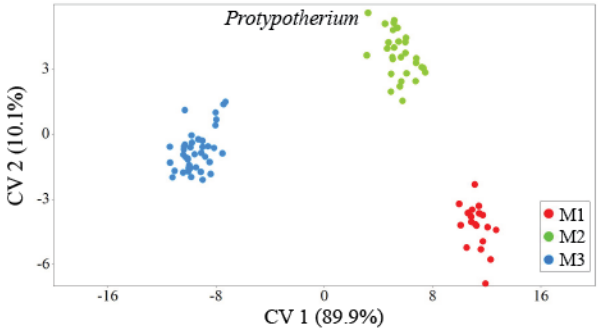

Figure. 16. CV axes of *Protypotherium* outline shape.

The CVA correctly classified the molar position for 100% of the *Paedotherium* and *Protypotherium* slices, while correctly classifying 96.7% of the *Hegetotherium* slices. Jackknifed cross-validation of the molar position CVA correctly classified 100% of *Paedotherium* and *Protypotherium* outlines, and reduced the *Hegetotherium* classification success rate to 93.3%.

CONCLUSION

Notoungulate specimens examined in this study can be reliably allocated to genus based solely on molar outline shape. By including the progression of outlines (from current to hypothesized future occlusal planes), this study negates the effect outline variability due to wear. There is a chance that a single outline may be misclassified, but when the entire population of (10) outlines from each tooth is considered, incorrect classification is unlikely. Although there is some overlap of ranges for various combinations of PC scores (Fig. 7-13) and CV scores (Fig. 14), when the totality of the data is taken into account, as seen in the quantitative CVA and MANOVA, the groups of molars are well identified. The results indicate that shape analysis of molar outlines, using computed tomography and elliptic Fourier analysis, is a promising method to discriminate between groups of hypselodont notoungulates. Further, once a molar is classified into the group to which it belongs, this method may be used to identify the tooth position of isolated teeth.

The current study is restricted to molars, but the methods developed here are likely applicable to hypselodont premolars as well. For taxonomic studies in which crown shape convergence is possible/suspected, crown outline analysis may provide a second test (after basic crown shape analysis) to determine the taxonomic placement of teeth. Increasing the sample size of scanned notoungulate teeth should ultimately permit hypselodont isolated teeth of uncertain taxonomic affinity to be identified. With a more robust database of hypselodont molars, correct classification can occur on the scale of hours. The rapid addition of worn cheek teeth to the outline database

would help to resolve numerous questions regarding the taxonomic affinity of notoungulate subgroups. Although the present study is limited to notoungulates, the analytical techniques are presumably applicable to a broad range of hypsodont taxa. Future work might include data from the premolars. The addition of basic outline geometric tooth measurements (e.g., length, width, circumference, and area) to the EFA would likely further increase the success of group discrimination.

REFERENCES

Adebowale, A., Nicholas, A., Lamb, J., & Naidoo, Y. (2012). Elliptic Fourier analysis of leaf shape in southern African *Strychnos* section *Densiflorae* (Loganiaceae). *Botanical Journal of the Linnean Society, 170*(4), 542-553.

Billet, G. (2011). Phylogeny of the Notoungulata (Mammalia) based on cranial and dental characters. *Journal of Systematic Palaeontology, 9*(4), 481-497.

Billet, G., Blondel, C., & De Muizon, C. (2009). Dental microwear analysis of notoungulates (Mammalia) from Salla (Late Oligocene, Bolivia) and discussion on their precocious hypsodonty. *Palaeogeography, Palaeoclimatology, Palaeoecology, 274*(1), 114-124.

Bourque, B. J., Morris, K., & Spiess, A. (1978). Determining the season of death of mammal teeth from archeological sites: a new sectioning technique. *Science, 199*(4328), 530-531.

Brett, C. E., & Baird, G. C. (1986). Comparative taphonomy: a key to paleoenvironmental interpretation based on fossil preservation. *Palaios,* 207-227.

Cifelli, R. L. (1993). The phylogeny of the native South American ungulates. *Mammal Phylogeny, 2*, 195-216.

Croft, D. A., Flynn, J. J., & Wyss, A. R. (2004). Notoungulata and Litopterna of the early Miocene Chucal fauna, northern Chile. *Fieldiana Geology*, 1-52.

Daegling, D. J., & Jungers, W. L. (2000). Elliptical Fourier analysis of symphyseal shape in great ape mandibles. *Journal of Human Evolution, 39*(1), 107-122.

Damuth, J., & Janis, C. M. (2011). On the relationship between hypsodonty and feeding ecology in ungulate mammals, and its utility in palaeoecology. *Biological Reviews, 86*(3), 733-758.

Dennis, J. C., Ungar, P. S., Teaford, M. F., & Glander, K. E. (2004). Dental topography and molar wear in *Alouatta palliata* from Costa Rica. *American Journal of Physical Anthropology, 125*(2), 152-161.

Fedorov, A., Beichel, R., Kalpathy-Cramer, J., Finet, J., Fillion-Robin, J. C., Pujol, S., Bauer, C., Jennings, D., Fennessy, F., Sonka, M., Buatti, J., Aylward, S.R., Miller, J.V., Pieper, Buatti, J., Kikinis, R. (2012). 3D Slicer as an image computing platform for the Quantitative Imaging Network. *Magnetic Resonance Imaging, 30*(9), 1323-1341.

Fisher, R. A. (1936). The use of multiple measurements in taxonomic problems. *Annals of Eugenics, 7*(2), 179-188.

Fortelius, M. (1985). Ungulate cheek teeth: developmental, functional, and evolutionary interrelations. *Acta Zoologica Fennica, 180,* 1-76.

Freeman, H. (1974). Computer processing of line-drawing images. *ACM Computing Surveys (CSUR), 6*(1), 57-97.

Gallina, P. A., & Apesteguía, S. (2011). Cranial anatomy and phylogenetic position of the titanosaurian sauropod *Bonitasaura salgadoi*. *Acta Palaeontologica Polonica, 56*(1), 45-60.

Hammer, Ø., Harper, D. A. T., & Ryan, P. D. (2001). PAST-PAlaeontological STatistics, ver. 1.89. *Palaeontologia electronica, 4*(1), 1-9.

Hâruta, O. (2011). Elliptic Fourier analysis of crown shapes in *Quercus petraea* trees. *Annals of Forest Research, 54*(1), 3.

Hopson, J. A. (1980). Tooth function and replacement in early Mesozoic ornithischian dinosaurs: implications for aestivation. *Lethaia, 13*(1), 93-105.

Iwata, H., & Ukai, Y. (2002). SHAPE: a computer program package for quantitative evaluation of biological shapes based on elliptic Fourier descriptors. *Journal of Heredity, 93*(5), 384-385.

Jardine, P. E., Janis, C. M., Sahney, S., & Benton, M. J. (2012). Grit not grass: concordant patterns of early origin of hypsodonty in Great Plains ungulates and Glires. *Palaeogeography, Palaeoclimatology, Palaeoecology, 365*, 1-10.

Jernvall, J. (2002). A gene network model accounting for development and evolution of mammalian teeth. *Proceedings of the National Academy of Sciences, 99*(12), 8116-8120.

Kaiser, T. M., & Brinkmann, G. (2006). Measuring dental wear equilibriums—the use of industrial surface texture parameters to infer the diets of fossil mammals. *Palaeogeography, Palaeoclimatology, Palaeoecology*, *239*(3), 221-240.

Kaiser, T. M., Müller, D. W., Fortelius, M., Schulz, E., Codron, D., & Clauss, M. (2013). Hypsodonty and tooth facet development in relation to diet and habitat in herbivorous ungulates: implications for understanding tooth wear. *Mammal Review*, *43*(1), 34-46.

Kendall, D. G. (1977). The diffusion of shape. *Advances in Applied Probability, 9*(3), 428-430.

Koenigswald, W. V. (2011). Diversity of hypsodont teeth in mammalian dentitions—construction and classification. *Palaeontographica Abteilung A, 294*, 63-94.

Kono, R. T. (2004). Molar enamel thickness and distribution patterns in extant great apes and humans: new insights based on a 3-dimensional whole crown perspective. *Anthropological Science, 112*(2), 121-146.

Kuhl, F. P., & Giardina, C. R. (1982). Elliptic Fourier features of a closed contour. *Computer Graphics and Image Processing, 18*(3), 236-258.

Kullmer, O., Benazzi, S., Fiorenza, L., Schulz, D., Bacso, S., & Winzen, O. (2009). Technical note: occlusal fingerprint analysis: quantification of tooth wear pattern. *American Journal of Physical Anthropology, 139*(4), 600-605.

Lord, C., Morat, F., Lecomte-Finiger, R., & Keith, P. (2012). Otolith shape analysis for three *Sicyopterus* (Teleostei: Gobioidei: Sicydiinae) species from New Caledonia and Vanuatu. *Environmental Biology of Fishes, 93*(2), 209-222.

Lucas, P. W., Casteren, A. V., Al-Fadhalah, K., Almusallam, A. S., Henry, A. G., Michael, S., Watzke, J., Reed, D. A., Diekwisch, T. G. H., Strait, D. S., Atkins, A. G. (2014). The role of dust, grit and phytoliths in tooth wear. *Annales Zoologici Fennici 51*(1), 143-152. Finnish Zoological and Botanical Publishing.

Luckett, W. P. (1993). An ontogenetic assessment of dental homologies in therian mammals In *Mammal Phylogeny* (eds. Szalay, F.S., Novacek, M.J., & McKenna, M.C.), pp. 182-204. Springer New York.

McNeel, R. (2010). Rhinoceros–NURBS Modeling for Windows (version 4). Available from: Seattle, WA, USA: McNeel North America www.rhino3d.com.

M'kirera, F., & Ungar, P. S. (2003). Occlusal relief changes with molar wear in *Pan troglodytes troglodytes* and *Gorilla gorilla gorilla*. *American Journal of Primatology, 60*(2), 31-41.

MacFadden, B. J. (1997). Origin and evolution of the grazing guild in New World terrestrial mammals. *Trends in Ecology & Evolution, 12*(5), 182-187.

Madden, R. H. (2014). *Hypsodonty in Mammals*. Cabridge, United Kingdom: Cambridge University Press.

McNaughton, S. J., & Tarrants, J. L. (1983). Grass leaf silicification: natural selection for an inducible defense against herbivores. *Proceedings of the National Academy of Sciences, 80*(3), 790-791.

Mebatsion, H. K., Paliwal, J., & Jayas, D. S. (2012). Evaluation of variations in the shape of grain types using principal components analysis of the elliptic Fourier descriptors. *Computers and electronics in agriculture, 80*, 63-70.

Ni, X., Flynn, J. J., & Wyss, A. R. (2010). The bony labyrinth of the early platyrrhine primate *Chilecebus*. *Journal of Human Evolution, 59(6)*, 595-607.

Olejniczak, A. J., Tafforeau, P., Feeney, R. N., & Martin, L. B. (2008). Three-dimensional primate molar enamel thickness. *Journal of Human Evolution, 54*(2), 187-195.

Pascual, R., & Jaureguizar, E. O. (1990). Evolving climates and mammal faunas in Cenozoic South America. *Journal of Human Evolution*, *19*(1), 23-60.

Paula Couto, C. (1952). Fossil mammals from the beginning of the Cenozoic in Brazil. Condylarthra, Litopterna, Xenungulata, and Astrapotheria. *Bulletin of the American Museum of Natural History, 99*, 355-394.

Rasband, W. S., & ImageJ, (1997). U. S. National Institutes of Health, Bethesda, Md, USA, http://imagej.nih.gov/ij/, 1997-2016.

Reguero, M. A., Candela, A. M., & Cassini, G. H. (2010). 24 Hypsodonty and body size in rodent-like notoungulates. *The paleontology of Gran Barranca: evolution and environmental change through the Middle Cenozoic of Patagonia*, 362.

Rensberger, J. M. (1973). An occlusion model for mastication and dental wear in herbivorous mammals. *Journal of Paleontology*, *47*(3), 515-527.

Renvoisé, E., & Michon, F. (2014). An Evo-Devo perspective on ever-growing teeth in mammals and dental stem cell maintenance. *Frontiers in Physiology, 5*(324).

Sanson, G. D., Kerr, S. A., & Gross, K. A. (2007). Do silica phytoliths really wear mammalian teeth?. *Journal of Archaeological Science, 34*(4), 526-531.

Shimomura, K., Horie, H., Sugiyama, M., Kawazu, Y., & Yoshioka, Y. (2016). Quantitative evaluation of cucumber fruit texture and shape traits reveals extensive diversity and differentiation. *Scientia Horticulturae*, *199*, 133-141.

Skogland, T. (1988). Tooth wear by food limitation and its life history consequences in wild reindeer. *Oikos*, 238-242.

Stirton, R. A. (1947). Observations on evolutionary rates in hypsodonty. *Evolution, 1*(1/2), 32-41.

Strauss, R. E., & Bookstein, F. L. (1982). The truss: body form reconstructions in morphometrics. *Systematic Biology*, *31*(2), 113-135.

Strömberg, C. A. (2011). Evolution of grasses and grassland ecosystems. *Annual Review of Earth and Planetary Sciences, 39*, 517-544.

Strömberg, C. A., Dunn, R. E., Madden, R. H., Kohn, M. J., & Carlini, A. A. (2013). Decoupling the spread of grasslands from the evolution of grazer-type herbivores in South America. *Nature Communications, 4*, 1478.

Suwa, G., & Kono, R. T. (2005). A micro-CT based study of linear enamel thickness in the mesial cusp section of human molars: reevaluation of methodology and assessment of within-tooth, serial, and individual variation. *Anthropological Science, 113*(3), 273-289.

Thompson, D. W. (1942). *On growth and form.* Cambridge, United Kingdom: Cambridge University Press

Tracey, S. R., Lyle, J. M., & Duhamel, G. (2006). Application of elliptical Fourier analysis of otolith form as a tool for stock identification. *Fisheries Research, 77*(2), 138-147.

Ungar, P. S. (2010). *Mammal teeth: origin, evolution, and diversity*. Baltimore, Maryland: Johns Hopkins University Press

Ungar, P. S. (2014). *Teeth: A Very Short Introduction*. Oxford, United Kingdom: Oxford University Press.

Ungar, P. S., & Sponheimer, M. (2011). The diets of early hominins. *Science, 334*(6053), 190-193.

Ungar, P. S., & Williamson, M. (2000). Exploring the effects of tooth wear on functional morphology: a preliminary study using dental topographic analysis. *Palaeontologia Electronica, 3*(1), 1-18.

van Dam, J. A., Fortuny, J., & van Ruijven, L. J. (2011). MicroCT-scans of fossil micromammal teeth: re-defining hypsodonty and enamel proportion using true volume. *Palaeogeography, Palaeoclimatology, Palaeoecology, 311*(1), 103-110.

van Nievelt, A. F., & Smith, K. K. (2005). To replace or not to replace: the significance of reduced functional tooth replacement in marsupial and placental mammals. *Paleobiology, 31*(2), 324-346.

Williams, S. H., & Kay, R. F. (2001). A comparative test of adaptive explanations for hypsodonty in ungulates and rodents. *Journal of Mammalian Evolution, 8*(3), 207-229.

Woodburne, M. O., Goin, F. J., Bond, M., Carlini, A. A., Gelfo, J. N., López, G. M., Iglesias, A., Zimicz, A. N. (2014). Paleogene land mammal faunas of South America; a response to global climatic changes and indigenous floral diversity. *Journal of Mammalian Evolution*, *21*(1), 1-73.

Young, I. T., Walker, J. E., & Bowie, J. E. (1974). An analysis technique for biological shape. I. *Information and Control*, *25*(4), 357-370.

Zelditch, M. (1998). Morphometric Tools for Landmark Data: Geometry and Biology. *BioScience, 48*(10), 855-858.

Zelditch, M. L., Swiderski, D. L., & Sheets, H. D. (2012). *Geometric morphometrics for biologists: a primer* (2nd ed.). San Diego, California: Academic Press.